



ICE LOAD ESTIMATION THROUGH COMBINED FINITE-DISCRETE ELEMENT SIMULATIONS

Janne Ranta, Arttu Polojärvi and Jukka Tuhkuri

Aalto University, School of Engineering, Department of Applied Mechanics

P.O. Box 14300, FI-00076 Aalto, Finland

Sustainable Arctic Marine and Coastal Technology (SAMCoT), Centre for Research-based

Innovation (CRI), Norwegian University of Science and Technology, Trondheim, Norway

e-mail: janne.ranta@aalto.fi

ABSTRACT

Ice load calculation is a complex task. The development of numerical modelling methods has made it possible to analyze ice-structure interaction problems in detail. In this paper we apply a 2D combined finite-discrete element method (FEM-DEM) to simulate ice interaction against an inclined rigid wall. We demonstrate how combined finite discrete element simulations can be used in studying maximum ice loads. We highlight the importance of running several virtual or real-life experiments when studying ice loads due to their stochasticity. Our focus is in simple statistical quantities and in the estimates of their errors.

INTRODUCTION

Ice loads are an important factor in the design of safe and efficient structures that operate on ice infested waters. Since ice loads are stochastic (Daley & al., 1998; Jordaan, 2001) they cannot be defined in an exact manner, and one has to use statistical methods in order to interpret measured or even simulated results. Here we study the statistics of ice loads in ice-structure interaction process based on simulations conducted using a 2D combined finite-discrete element method (FEM-DEM).

This paper aims to demonstrate a powerful way to use simulations in studying statistics of maximum ice loads: we can run a large number of virtual experiments to produce a large data set with full control on parameters. We study the sample-size-dependent error in the prediction of maximum load values. Our findings suggest that sometimes simulation-based statistical studies could be used to improve predictions on full-scale ice loads. Our study is based on few fairly simple statistical quantities that describe maximum loads.

We first introduce our simulations, the used statistical quantities, and the basis of our analysis. Then we show that our simulated data is in fair agreement to full-scale ice load data, and analyze its statistical properties. Before concluding the paper we discuss our results from the aspect of experimentation.

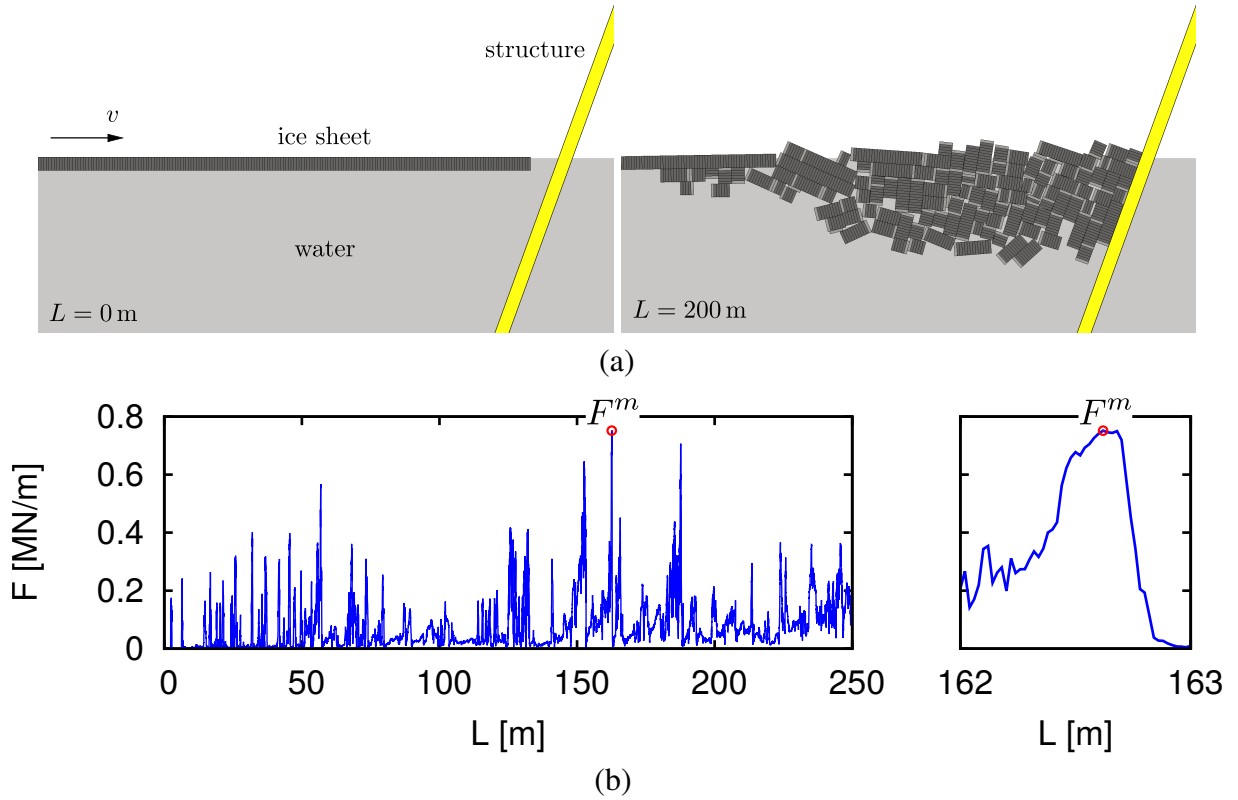


Figure 1: Typical simulated ice-structure interaction process: snapshots from a simulation in its initial position and after 200 m of pushed ice L , and (b) a typical horizontal force F record with the maximum force F^m indicated.

SIMULATIONS AND STATISTICS

Our 2D FEM-DEM simulations had a floating ice sheet pushed against an inclined rigid structure. The ice sheet had a constant velocity. Figure 1 a shows two snapshots from a simulation. We performed the simulations using an in-house code of the Aalto University ice mechanics group. The DEM part of the code is in align with the model published by Hopkins (1992). The FEM modelling of the ice sheet is presented in detail in Paavilainen & al. (2009). Paavilainen & al. (2011) and Paavilainen and Tuhkuri (2012, 2013) validated the model against full- and model-scale data, and studied the mechanics of the ice-structure interaction process with it.

The simulated ice sheet was formed by discrete elements connected to each other with Timoshenko beam elements. The beam elements were linearly elastic until a chosen failure criterion was met and then went through an energy dissipating cohesive softening leading to failure when further loaded. As described in Paavilainen & al. (2009), the beam element unites with the line connecting the discrete elements centroids and its nodes have the same degrees of freedom as the discrete elements it is combining, two displacements and a rotation at each node. The properties of the ice sheet were homogeneous. Discrete elements were used to treat interactions between the different parts of the system, including contacts between the ice blocks and the contacts between the ice and the structure. Figure 1 b shows a typical horizontal load F record from a simulation with the maximum horizontal load F^m indicated. The close-up of the the record shows, that a typical F^m was not caused by a short impact. For example, the time inter-

val in the case of the close-up is 20 s. Table 1 summarizes the simulation parameters, which we for the most parts chose based on Timco and Weeks (2010).

The results of this paper are based on 110 simulations with two different plastic limit σ_p values. We chose to vary σ_p , since earlier work in Paavilainen and Tuhkuri (2012) suggested it might affect F^m values with thick ice. Other parameters were constant in all simulations. With both σ_p values we ran 55 repeated simulations. Each simulation in a set of repeated simulations had slightly different initial vertical velocity on the right end of the ice sheet, which caused a difference in the state of the simulation after a while. Paavilainen and Tuhkuri (2012) showed that only a very small change in the simulation parameter values was enough to cause the simulated system to end up in the different state. In the repeated simulations, a fraction of a mm/s difference in the initial vertical velocity of the tip of the ice sheet was needed to cause difference in F records, and consequently F^m values, between the simulations.

We studied the sample-size-dependent error in the prediction of maximum load values. We based our study on two simple statistical quantities describing the F^m values: their mean \bar{x} and the standard deviation s . Using these, we first defined the required number N of experiments for different levels of confidence and accuracy. An estimate for N can be shown to be given by (Ryan, 2013)

$$N = 10000c_v^2 \left(\frac{a}{b}\right)^2 \quad (1)$$

where $c_v = s/\bar{x}$ and parameters a and b are chosen based on wanted levels of confidence and error, respectively. When analysing the error, we chose $a = 1.96$ to yield 95 % confidence level and investigated the change in the value b (in percentages) with various N values. It should be noted that the previous equation with $a \neq 1$ assumes that the underlying data is normally distributed and leads only to a rough estimate for b if N is small.

We also calculated upper and lower error estimates for \bar{x} values using a distribution independent bootstrapping procedure (Efron, 1979). This way we were not only able to improve the quality of our statistical figures, but also estimate the validity of Equation 1 with various N values. The bootstrapping procedure is based on random sampling with replacement. In our case with the

Table 1: Summary of the simulation parameter values.

| Variable description | Unit | Value | Variable description | Unit | Value |
|----------------------------|-------------------|-------|---------------------------------|-------------------|----------|
| General | | | Contact | | |
| Gravitational acceleration | m/s ² | 9.81 | Plastic limit (σ_p) | MPa | 1.0, 2.0 |
| Ice sheet velocity | m/s | 0.05 | Friction coeff. (ice-ice) | | 0.1 |
| Drag coefficient | | 2.0 | Friction coeff. (ice-structure) | | 0.1 |
| Ice | | | Water | | |
| Thickness | m | 1.25 | Density | kg/m ³ | 1010 |
| Effective modulus | GPa | 4 | Structure | | |
| Poisson's ratio | | 0.3 | Slope angle | deg | 70 |
| Density | kg/m ³ | 900 | | | |
| Tensile strength | kPa | 600 | | | |
| Shear strength | kPa | 600 | | | |

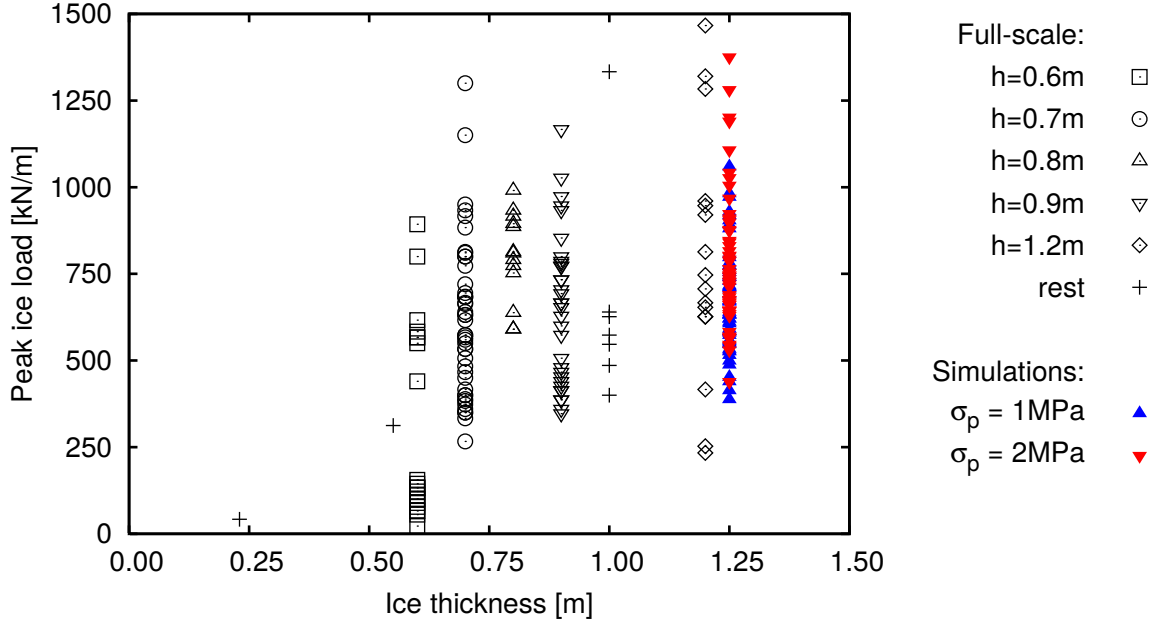


Figure 2: Maximum load F^m values from our simulations with different plastic limit σ_p values (red and blue markers) and from Timco and Johnston (2004) (black markers) plotted against ice thickness h . The marker styles indicate datapoints included into the datasets used in Figures 3 and 4 for each h . Figure also shows datapoints (rest) for h values not included in the analysis of error due to low number ($N < 10$) of samples.

simulations, the source of these random samples was the set of 55 simulated F^m observations for both σ_p values. The number of random samples (so-called bootstrap samples) in our case was 10^4 . We also tested to use 10^6 random samples but found no difference in results with the accuracy of two significant digits.

RESULTS AND ANALYSIS

The maximum load F^m data from the simulations was in agreement with full-scale observations as Figure 2 shows. The figure has F^m data from our simulations and the observations on maximum ice loads acting on Molikpaq structure (Timco and Johnston, 2004) plotted against the ice thickness h . As this paper includes simulations with only one h value, the simulation results fall onto a vertical line at $h = 1.25$ m. We note that a more thorough comparison (albeit with lower number of simulations in each repeated set) done in Paavilainen & al. (2011) showed that the peak load values from the simulations are in agreement with the data in Timco and Johnston (2004) with various h values.

Next we calculated mean values \bar{x} and standard deviations s for maximum load samples in Figure 2 and did an error analysis based on Equation 1. The errors of the \bar{x} values can be roughly estimated from Figure 3. The figure shows data points for a number of data sets: each simulated set has a unique h and σ_p and each full-scale set a unique h value. Only the full-scale data sets for h values with number of samples $N > 10$ are used. The marker styles indicate the correspondence between the data points and sets of Figures 2 and 3, respectively. The number

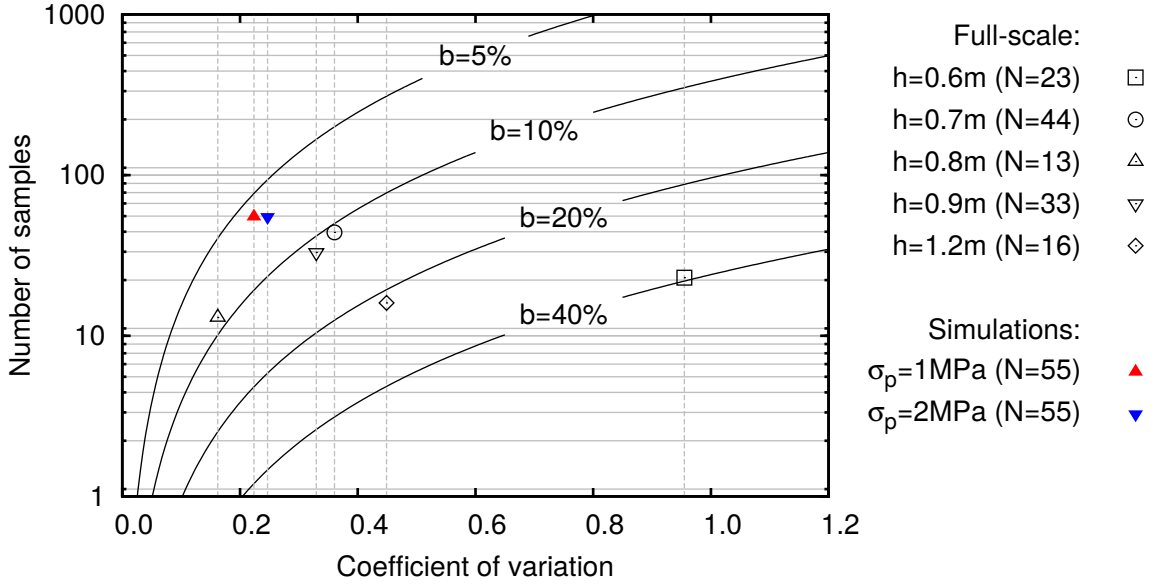


Figure 3: Number N of samples plotted against $c_v = s/\bar{x}$, where \bar{x} is the mean of maximum load values and s their standard deviation, from our simulations and Timco and Johnston (2004). The black lines show the contours for error b (in percentages) defined using Equation 1 and assuming confidence interval of 95 %. The dashed vertical lines can be used as a visual aid for defining the N needed for different levels of error b for constant c_v .

of samples in a data set gives the N value for each point in Figure 3, whereas the c_v value of each point is based on \bar{x} and s value of the corresponding set. Error of \bar{x} can be estimated from the figure using the Equation 1 based contours of error b .

Three preliminary findings Figure 3 shows are: (1) the simulated and full-scale data mostly show similar c_v values, (2) simulations may be an effective tool for improving \bar{x} estimates, since the number N needed for a chosen error b increases rapidly with c_v , and (3) the full-scale data does not show any correlation between h and c_v . Finding (1) is shown by the simulated data being on the same regime of the plot with full-scale data, excluding the full-scale data point corresponding to $h = 0.6$ m. This data point likely suffers from the fairly low number of samples in the intermediate load range, which is undeniably the problem with some other full-scale data points as well.

Finding (2) together with (1) suggests that the simulations could be used to get improved ice load estimates. Compared to experiments it is easy to achieve the high N needed for accuracy in the simulations, while simultaneously having control on parameters. Finding (3) makes statistical analysis on ice loads at least a bit simpler in general, since in case c_v would correlate with h , generating statistical models for ice loads would become (even more) challenging. We are aware that the low N for full-scale observations for some h values may partly affect the validity of these findings. Hence, more full-scale data would be needed.

Table 2 shows the mean values \bar{x} , standard deviations s and coefficients of variation c_v from the simulations and for data set $h = 0.7$ m from Timco and Johnston (2004). This data set was chosen as it had the highest number of samples ($N = 44$). The table also shows estimated 95% confidence intervals for these quantities. These confidence intervals are a result of the bootstrapping process and are not dependent on the distribution of the data. For the later discussion,

we already note that the upper confidence interval c_v^+ for the coefficient of variation can be substituted to Equation 1, which then can be used to roughly estimate the upper bound for the error b .

Results in Table 2 show that mean maximum load \bar{x} increases from 665 kN to 777 kN as σ_p increases from 1 MPa to 2 MPa. Interestingly an increase is seen in the value of standard deviation s also but it is less clear than in the case of \bar{x} . This may be important and might need to be taken into account when analyzing the ice load data statistically or when parameter effects on ice loads are considered. The c_v values on the other hand remain fairly constant and are smaller than in the case of experimental data. The c_v^- and c_v^+ values are not symmetrical with respect to c_v in any case, which indicates that none of the data sets is strictly normally distributed. Some consequences of this are briefly addressed in the next section. Comparing \bar{x} value based on full-scale observations to simulated \bar{x} is not relevant here, since the full-scale data set had different ice thickness h than the simulations due to aforementioned issue with the number of samples.

DISCUSSION

From the aspect of peak ice load estimation, it is interesting to discuss the change in the uncertainty of maximum load estimates as the number N of samples increases, or in other words, to try answer to the question: what is the error if we can only make a limited number N of samples, and how would this error change if we could increase N ? Figure 4 presents the results of our preliminary analysis on this issue by showing 95 % error margin for mean maximum load \bar{x} plotted against the number of samples N for simulation and full-scale data (case $h = 0.7$ m).

We calculated the error margins of Figure 4 with the similar bootstrapping procedure as described above, only this time the procedure was executed for randomly chosen sub-samples of the original data. Each data point of the figure is based on 10^4 random sub-samples having N indicated by the horizontal axis. In addition, the figure shows the upper bound for the error b for the case of the simulations with $\sigma_p = 2$ MPa and full-scale data. As was mentioned above, these upper bounds are achieved using Equation 1 and c_v^+ values of Table 2.

Figure 4 shows three important features related to maximum ice-loads in ice-structure interaction process: (1) the error margins in all cases are large with small N , (2) they drop drastically as N increases, and (3) the N needed for reasonable error margins is fairly high from the aspect of peak ice load estimation. Feature (1) is shown by the fact that with $N = 5$ the simulated data show higher than 30 % and full-scale higher than 50 % error. It is not exceptional to base statis-

Table 2: Mean values \bar{x} , standard deviations s and coefficients of variations c_v with corresponding lower and upper 95% bootstrap confidence intervals (superscripts $-$ and $+$, respectively). Full-scale values are based on data set for $h = 0.7$ m from Timco and Johnston (2004).

| | \bar{x} | \bar{x}^- | \bar{x}^+ | s | s^- | s^+ | c_v | c_v^- | c_v^+ |
|-------------------------|-----------|-------------|-------------|-------|-------|-------|-------|---------|---------|
| Sim $\sigma_p = 1$ Mpa: | 665.0 | 627.0 | 705.0 | 150.0 | 119.0 | 175.0 | 0.225 | 0.183 | 0.26 |
| Sim $\sigma_p = 2$ Mpa: | 777.0 | 730.0 | 827.0 | 185.0 | 136.0 | 227.0 | 0.239 | 0.181 | 0.284 |
| Full-scale: | 620.0 | 556.0 | 687.0 | 223.0 | 166.0 | 274.0 | 0.36 | 0.278 | 0.429 |

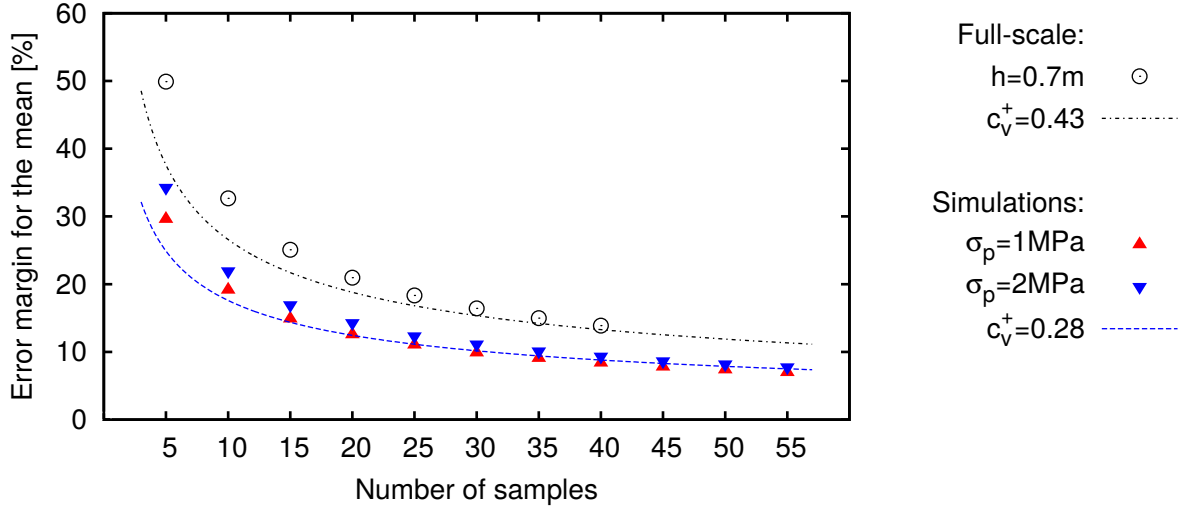


Figure 4: Maximum error values as function of N .

tical quantities in the experiments to ice load data sets having $N = 5$. The error is (2) initially observed to drop fast, but (3) to get down to, for example 20 % error margin, approximately 25 full-scale samples is needed. This N value is often challenging to reach in an experimental study, in both, model or full-scale. We note here that the data in model scale experiments might show different error than the full-scale data used here, in which case N needed for certain error also changes.

Figure 4 shows the two different error estimates, b is indicated by the lines and error margin based on bootstrapping by the markers, which deviate for all the data shown. This again indicates that the underlying data is not strictly normally distributed. The deviation in the error estimates is fairly large with N as the figure shows. The distribution thus may have a role in estimating the error with small N , which is often the case in the experiments but can be avoided in the simulations. Further challenge arises from the fact that data sets with small N do not allow a study on the distribution of the set.

Finally the data in Figure 4 shows that the simulations had smaller error margin than the full-scale observations. Partly this is again due to the control on parameters in the simulations, since in between each full-scale observation, there is practically always some variation in the parameters. Smaller error in the simulations when compared to full scale observations would be also expected due to the larger sample size for the simulated data ($N = 55$) when compared to full-scale observations ($N = 44$ at maximum).

CONCLUSIONS

In this paper we studied the prediction of maximum load values in ice-structure interaction process. Study was based on 2D FEM-DEM simulations. We aimed to demonstrate the applicability of such simulations in a statistical study on ice loads. Our preliminary observations presented and discussed above are:

- The maximum ice load F^m values in our simulations and in full-scale tend to show fairly high standard deviation to mean value ratios, which lead to high number of

samples N needed for accurate predictions on ice loads (see Figure 3).

- A tolerable upper bound for the error in prediction of F^m can be found, but with such high N values, that they might not be attainable in the real-life experiments so that ice material parameters stay constant (see Figure 4).
- Simulations might be a powerful tool to apply in studies on statistics of ice loads, since the high N values needed for accuracy can be reached while maintaining full control on the parametrization of the problem.

We will have a future study on the distribution of our maximum load F^m data, since the data here was found to be not strictly normally distributed. The number of samples in the experiments or full-scale is often insufficient to conclude on the distribution of it. One should notice here that the bootstrapping does not set any limitations on the distribution of the underlying data, so that the observations on upper bound of the error in Figure 4 remain valid, even if our data was not normally distributed.

ACKNOWLEDGMENTS

The authors wish to acknowledge the support from the Research Council of Norway through the Centre for Research-based Innovation SAMCoT and the support from all SAMCoT partners.

REFERENCES

- Daley, C.G., Tuhkuri, J. and Riska, K., 1998. The role of discrete failures in local ice loads. Cold Regions Science and Technology, 27, pp. 197-211.
- Efron, B., 1979. Bootstrap methods: Another look at the Jackknife. The Annals of Statistics, Vol 7., No. 1, pp. 1-26.
- Hopkins, M., 1992. Numerical Simulation of Systems of Multitudinous Polygonal Blocks. Technical Report 92-22. Cold Regions Research and Engineering Laboratory (CRREL), 69 p.
- Jordaan, I.J., 2001. Mechanics of ice-structure interaction. Engineering Fracture Mechanics, 68, pp. 1923-1960.
- Paavilainen, J., Tuhkuri, J. and Polojärvi, A., 2009. 2D Combined finite-discrete element method to model multi-fracture of beam structures. Engineering Computations, Volume 26, issue 6, pp. 578-598.
- Paavilainen, J., Tuhkuri, J. and Polojärvi, A., 2011. 2D numerical simulations of ice rubble formation process against in inclined structure. Cold Regions Science and Technology, 68, pp. 20-34.
- Paavilainen, J. and Tuhkuri, J., 2012. Parameter effects on simulated ice rubbing forces on a wide sloping structure. Cold Regions Science and Technology, 81, pp. 1-10.

- Paavilainen, J. and Tuhkuri, J., 2013. Pressure distributions and force chains during simulated ice rubbing against sloped structures. *Cold Regions Science and Technology*, 85, pp. 157-174.
- Ryan, T.P., 2013. Sample size determination and power. Wiley, 404 p., ISBN 978-1-118-43760-5.
- Timco, G.W. and Johnston, M., 2004. Ice loads on the caisson structures in the Canadian Beaufort Sea. *Cold Regions Science and Technology*, 38, pp. 185-209.
- Timco, G. and Weeks, W., 2010. A review of the engineering properties of sea ice. *Cold Regions Science and Technology*, 60, pp. 107-129.